TECHNICAL RESEARCH REPORT

Modeling and Control of a Magnetostrictive Actuator

by Xiaobo Tan, John S. Baras

CDCSS TR 2002-3
(ISR TR 2002-8)

The Center for Dynamics and Control of Smart Structures (CDCSS) is a joint Harvard University, Boston University, University of Maryland center, supported by the Army Research Office under the ODDR&E MURI97 Program Grant No. DAAG55-97-1-0114 (through Harvard University). This document is a technical report in the CDCSS series originating at the University of Maryland.

Web site http://www.isr.umd.edu/CDCSS/cdcss.html

CDC02-REG0909

Modeling and Control of a Magnetostrictive Actuator

Xiaobo Tan, John S. Baras
Institute for Systems Research and
Department of Electrical and Computer Engineering
University of Maryland, College Park, MD 20742 USA
{xbtan, baras}@isr.umd.edu

Abstract

The rate-dependent hysteresis existing in magnetostrictive actuators presents a challenge in control of these actuators. In this paper we propose a novel dynamical model for the hysteresis based on the work of Venkataraman and Krishnaprasad. The model features the coupling of the Preisach operator with an ordinary differential equation. We prove the well-posedness of the model and study identification methods for the model. An inverse control scheme is developed based on the dynamical model. The effectiveness of the identification and inverse control schemes is demonstrated through experimental results.

1 Introduction

Smart materials, such as magnetostrictives, piezoelectrics, electroactive polymers (EAPs), shape memory alloys (SMAs), electrorheological (ER) fluids and magnetorheological (MR) fluids, all display certain coupling phenomena between applied electromagnetic/thermal fields and their mechanical/rheological properties. Smart actuators and sensors made of these materials can be built into structures, often called *smart structures*, with the ability to sense and respond to environmental changes to achieve desired goals. However the rate-dependent hysteretic behavior existing in smart materials makes effective use of these actuators and sensors quite challenging.

A fundamental idea in coping with hysteresis is to formulate the mathematical model of hysteresis and use inverse compensation to cancel out the hysteretic effect. This idea can be found in [1, 2, 3, 4, 5, 6], to name a few. There have been a few monographs devoted to modeling of hysteresis and study of dynamical systems with hysteresis [7, 8, 9, 10]. Hysteresis models can be roughly classified into physics-based models [11, 12, 13] and phenomenological models. The most popular phenomenological hysteresis model used in control of smart actuators has been the Preisach model [1, 5, 6, 14, 15, 16, 17]. A similar type of operator, called Krasnosel'skii-Pokrovskii (KP) operator has also been used [4, 18]. Although the Preisach model generally does not provide physical insight into the problem, it provides a means of developing phenomenological models that are capable of producing behaviors similar to physical systems (see Mayergoyz [8] for an excellent exposition).

In this paper, we study control of a magnetostrictive actuator. Magnetostriction is the phenomenon of strong coupling between magnetic properties and mechanical properties of some ferromagnetic materials (e.g., Terfenol-D): strains are generated in response to an applied magnetic field, while conversely, mechanical stresses in the materials produce measurable changes in magnetization. Magnetostrictive actuators have applications in micro-positioning, robotics, ultrasonics, vibration control, etc. Figure 1 shows a sectional view of a Terfenol-D actuator manufactured by ETREMA Products, Inc. By varying the current in the coil, we vary the magnetic field in the Terfenol-D rod and thus control the motion of the rod head.

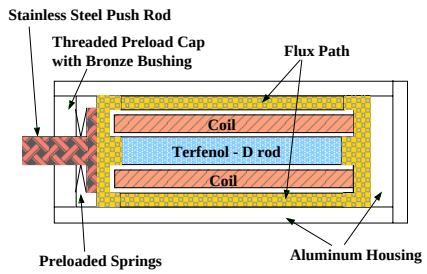

Figure 1: Sectional view of a Terfenol-D actuator [19](Original source: Etrema Products Inc.).

The hysteretic behavior of a magnetostrictive actuator at low frequencies (typically below 5 Hz) is rate-independent: roughly speaking, the shape of the hys-

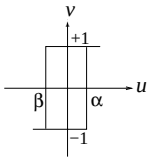

Figure 2: The elementary Preisach hysteron

teresis loop does not depend on the frequency of the input. This is no longer the case when the operating frequency gets high, due to the eddy current effect and the magnetoelastic dynamics of the magnetostrictive rod. The (rate-independent) Preisach operator alone is not capable of modeling the rate-dependent hysteresis. Based on the work of Venkataraman and Krishnaprasad, we propose a novel dynamical model for a thin magnetostrictive actuator, featuring the coupling of the Preisach operator and an ordinary differential equation.

The remainder of the paper is organized as follows. Section 2 provides an introduction to the Preisach operator. In Section 3 we describe the new model and prove its well-posedness. Parameter identification methods are discussed in Section 4 along with the experimental results. In Section 5 we present an inverse control scheme based on the dynamical model and test its performance in an open-loop tracking experiment. Concluding remarks are provided in Section 6.

2 The Preisach Model

Consider a simple hysteretic element (relay) shown in Figure 2. The relationship between the "input" variable u and the "output" variable v at each instant of time t can be described by:

$$\begin{cases} v = +1 & \text{if} \quad u > \alpha, \\ v = -1 & \text{if} \quad u < \beta, \\ v & \text{remains unchanged if} \quad \beta \le u \le \alpha. \end{cases} . \qquad (1)$$

Call the operator relating $u(\cdot)$ to $v(\cdot)$ as $\hat{\gamma}_{\beta,\alpha}[\cdot]$, where we now view the input and output variables as functions of time. Note to be precise, $\hat{\gamma}_{\beta,\alpha}$ also depends on the initial value of v. This operator is sometimes referred to as an *elementary Preisach hysteron* since it is a basic block from which the Preisach operator $\Gamma[\cdot]$ will be constructed. The output of the Preisach operator is defined as:

$$y(t) = \Gamma[u](t) = \int\int_{\alpha \ge \beta} \mu(\beta,\alpha)\hat{\gamma}_{\beta,\alpha}[u](t)d\beta d\alpha, \quad (2)$$

where $\mu(\cdot,\cdot)$ is a weighting function, called the *Preisach measure*.

The memory effect of the Preisach operator can be captured by curves in the *Preisach plane*. The Preisach plane is defined as $P \triangleq \{(\beta,\alpha)|\alpha \ge \beta\}$, and each $(\beta,\alpha) \in P$ is identified with the hysteron $\hat{\gamma}_{\beta,\alpha}$. At each time instant t, P can be divided into two regions:

$$P_-(t) \triangleq \{(\beta,\alpha) \in P| \quad \text{output of } \hat{\gamma}_{\beta,\alpha} \text{ at } t \text{ is} -1\},$$
$$P_+(t) \triangleq \{(\beta,\alpha) \in P| \quad \text{output of } \hat{\gamma}_{\beta,\alpha} \text{ at } t \text{ is} +1\},$$

so that $P = P_-(t) \cup P_+(t)$ at all times. Equation (2) can be rewritten as:

$$y(t) = \int\int_{P_+(t)} \mu(\beta,\alpha)d\beta d\alpha - \int\int_{P_-(t)} \mu(\beta,\alpha)d\beta d\alpha. \qquad (3)$$

In most cases of interest, each of P_- and P_+ is a connected set, and the output of the Preisach operator is determined by the boundary between P_- and P_+. The boundary is also called the *memory curve*, since it provides information about the state of any hysteron. The memory curve ψ_0 at $t = 0$ is called the *initial memory curve* and it represents the initial condition of the Preisach operator. Hereafter we will put ψ_0 explicitly as one of the arguments of Γ to emphasize the dependence of the Preisach operator on ψ_0.

Theorem 1 summarizes some basic properties of the Preisach operator, see, e.g., [9].

Theorem 1: *Let μ be the Preisach measure and $u, u_1, u_2 \in C([0,T])$, and let ψ_0 be some initial memory curve.*

1. **[Rate Independence]** *If $\phi : [0,T] \to [0,T]$ is an increasing homeomorphism, then $\Gamma[u \circ \phi, \psi_0](t) = \Gamma[u,\psi_0](\phi(t))$, $\forall t \in [0,T]$, where "$\circ$" denotes composition of functions.*
2. **[Strong Continuity]** *If μ is a finite Borel measure on P, and $\int_{-\infty}^{\infty} \mu(\beta,\alpha')d\alpha' = \int_{-\infty}^{\infty} \mu(\beta',\alpha)d\beta' = 0$, $\forall \beta,\alpha$, (i.e., the measure is nonsingular), then $\Gamma[\cdot,\psi_0] : C([0,T]) \to C([0,T])$ is strongly continuous (in the* sup *norm).*
3. **[Piecewise Monotonicity]** *Assume $\mu \ge 0$. If u is either nondecreasing or noninreasing in some interval in $[0,T]$, then so is $\Gamma[u,\psi_0]$.*
4. **[Order Preservation]** *Assume $\mu \ge 0$. If $u_1 \le u_2$ in $[0,T]$, then $\Gamma[u_1,\psi_0] \le \Gamma[u_2,\psi_0]$ in $[0,T]$.*

3 A Dynamical Model for the Hysteresis

Venkataraman and Krishnaprasad proposed a bulk magnetostrictive hysteresis model based on energy balancing principles [12, 19]. The model has a cascaded

structure as shown in Figure 3. W takes care of the $M-H$ hysteresis and the eddy current loss, where M and H denote the bulk magnetization and the magnetic field (assumed uniform) along the rod direction, respectively. The eddy current loss was considered by connecting a resistor R_{eddy} in parallel with a hysteretic inductor, where the $M-H$ hysteresis was described by a low dimensional ferromagnetic hysteresis model [12, 19]. $G(s)$ is a second order linear system modeling the magnetoelastic dynamics of the rod.

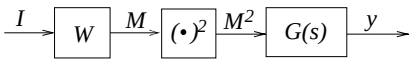

Figure 3: Model structure of a magnetostrictive actuator

Based on the work of Venkataraman and Krishnaprasad, we propose a new dynamical model where the Preisach operator Γ is used to model the $M-H$ hysteresis. The W block now reads

$$\begin{cases} \dot{H}(t)+\dot{M}(t)=\frac{R_{eddy}}{\mu_0 N_m A_m}(I(t)-\frac{H(t)}{c_0}) \\ M(t)=\Gamma[H(\cdot),\psi_0](t) \end{cases}, \quad (4)$$

where I is the input current, μ_0 is the permeability of vacuum, N_m is the number of turns of the coil, A_m is the cross sectional area of the rod, and c_0 is the coil factor (the constant relating the current to the magnetic field it generates). $G(s)$ has a state space representation [12, 19](after some manipulations):

$$\ddot{y}(t)+2\xi\omega_0\dot{y}(t)+\omega_0^2 y(t)=\frac{\omega_0^2 l_m\lambda_s}{M_s^2}M^2(t), \quad (5)$$

where y is the displacement, $\omega_0=2\pi f_0$, f_0 is the first resonant frequency of the actuator, ξ is the damping coefficient, l_m is the length of the rod, λ_s is the saturation magnetostriction and M_s is the saturation magnetization.

Note if we set derivatives in (4) and (5) to zero, the dynamical model degenerates to the static hysteresis model used in [5]:

$$\begin{cases} H(t)=c_0 I(t) \\ M(t)=\Gamma[H(\cdot),\psi_0](t) \\ y(t)=\frac{l_m\lambda_s}{M_s^2}M^2(t) \end{cases}. \quad (6)$$

Eq.(4) involves time derivatives of both H and M. It is well known that, in general, a Preisach operator does not map C^1 into C^1. Hence we will interpret (4) in the sense of Carathéodory [20]. Some partial differential equations with hysteretic operators appearing in the principal parts have been studied, see [9, 10] and references therein. Existence and uniqueness proof of solutions to equations of the form

$$\dot{y}=f(t,y,\Gamma(z)),\ z=g(y), \quad (7)$$

can be found in [10]. To our best knowledge, no such result has been published for equations like (4).

Theorem 2: *If the Preisach measure μ is a nonnegative, nonsingular, finite Borel measure, and $I(\cdot)$ is piecewise continuous, then for any ψ_0, for any $T>0$, there exists a unique pair $\{H(\cdot),M(\cdot)\}\in C([0,T]\times C([0,T])$ satisfying (4) almost everywhere.*

Proof. 1. We first show the existence. From ψ_0, one can evaluate initial values $H(0)$ and $M(0)$. Eq.(4) is equivalent to the following: $\forall t\in[0,T]$,

$$\begin{cases} H(t)+M(t)=H(0)+M(0)+\int_0^t c_1(I(s)-\frac{H(s)}{c_0})ds \\ M(t)=\Gamma[H(\cdot),\psi_0](t) \end{cases} \quad (8)$$

where we have defined $c_1=\frac{R_{eddy}}{\mu_0 N_m A_m}$. As in the proof of existence for the heat equation with hysteresis in [10], we use an Euler polygon method to approximate (4): for $N>0$ and $h_N=\frac{T}{N}$, solve consecutively

$$\begin{cases} \frac{H_N^{(m+1)}-H_N^{(m)}}{h_N}+\frac{M_N^{(m+1)}-M_N^{(m)}}{h_N}=c_1(I_N^{(m)}-\frac{H_N^{(m)}}{c_0}) \\ M_N^{(m+1)}=\Gamma[H_N^{(m+1)},\psi_m] \end{cases}, \quad (9)$$

for $0\le m\le N-1$, with $H_N^{(0)}=H(0)$, $M_N^{(0)}=M(0)$, $I_N^{(m)}=\frac{1}{h_N}\int_{mh_N}^{(m+1)h_N}I(s)ds$, and ψ_m the memory curve corresponding to $H_N^{(m)}$. With a little bit notation abuse, we tacitly understand that the input of Γ is changed monotonically from $H_N^{(m)}$ to $H_N^{(m+1)}$. Since under the assumption, $\Gamma[\cdot,\psi_m]$ is strongly continuous and piecewise monotone (Theorem 1), (9) admits a unique solution for $H_N^{(m+1)}$ and thus for $M_N^{(m+1)}$. Furthermore, by piecewise monotonicity, $H_N^{(m+1)}-H_N^{(m)}$ and $M_N^{(m+1)}-M_N^{(m)}$ have the same sign, from which we have

$$\begin{aligned} |\frac{H_N^{(m+1)}-H_N^{(m)}}{h_N}| &\le c_1|I_N^{(m)}-\frac{H_N^{(m)}}{c_0}| \\ &\le c_1(|I_N^{(m)}|+\frac{|H_N^{(m)}|}{c_0}). \end{aligned} \quad (10)$$

Since $I(\cdot)$ is piecewise continuous, we have $\forall m$, $I_N^{(m)}\le C_I$, with $C_I>0$ independent of N. From (10), we can get

$$\begin{aligned} H_N^{(m)} &\le (1+\frac{c_1 T}{c_0 N})^N(H(0)+c_0C_I)-c_0C_I \\ &< e^{\frac{c_1T}{c_0}}(H(0)+c_0C_I)-c_0C_I=:C, \end{aligned} \quad (11)$$

for all m, and C is independent of N. Boundness of $M_N^{(m)}$ is a natural consequence of (11).

We obtain $H_N(\cdot),M_N(\cdot)\in C([0,T])$ by linearly interpolating $\{H_N^{(m)}\}$ and $\{M_N^{(m)}\}$, i.e., $H_N(t)=\tau H_N^{(m)}+(1-\tau)H_N^{(m+1)}$, for $t=(m+\tau)h_N$, $0\le\tau\le1$, and analogously for $M_N(\cdot)$. Combining (10) and (11) we see

that $H_N(\cdot)$ is Lipshitz continuous with Lipshitz constant $L = c_1(C_I + \frac{C}{c_0})$ and the same is true for $M_N(\cdot)$. Therefore $\{H_N(\cdot)\}_{N\geq 1}$ is a family of equicontinuous, equibounded functions, and by Ascoli-Arzelá Theorem, $H_N(\cdot) \to \widetilde{H}(\cdot) \in C([0,T])$ uniformly. It's easy to see that $\widetilde{H}(\cdot)$ is also Lipshitz continuous and thus differentiable almost everywhere. Similarly $M_N(\cdot) \to \widetilde{M}(\cdot) \in C([0,T])$ uniformly.

Now define $e_N(t) = \dot{H}_N(t) + \dot{M}_N(t) - c_1(I(t) - \frac{H_N(t)}{c_0})$. By definitions of $H_N(\cdot)$ and $M_N(\cdot)$, we derive that $e_N(t) = c_1(I_N^{(m)} - I(t)) - \frac{c_1(H_N^{(m)} - H_N(t))}{c_0}$, for $t \in (mh_N, (m+1)h_N)$. Integrate

$$\dot{H}_N(t) + \dot{M}_N(t) = c_1(I(t) - \frac{H_N(t)}{c_0}) + e_N(t),$$

from 0 to t, and let $N \to \infty$, one can show $\widetilde{H}(\cdot)$ and $\widetilde{M}$ satisfy the first part of (8) and we are left to show $\widetilde{M}(t) = \Gamma[\widetilde{H}(\cdot), \psi_0](t)$, $\forall t \in [0,T]$.

Let $\overline{M}_N = \Gamma[H_N(\cdot), \psi_0]$. By strong continuity of Γ, $\overline{M}_N \to \Gamma[\widetilde{H}(\cdot), \psi_0]$ since $H_N(\cdot) \to \widetilde{H}(\cdot)$. Furthermore we have $\overline{M}_N(mh_N) = M_N(mh_N)$, $0 \leq m \leq N$. This together with piecewise monotonicity of Γ enables us to conclude $\sup_{t\in[0,T]} |M_N(t) - \overline{M}_N(t)| \leq Lh_N$. Therefore $\{M_N\}$ and $\{\overline{M}_N\}$ have the same limit, i.e., $\widetilde{M}(t) = \Gamma[\widetilde{H}(\cdot), \psi_0](t)$, $\forall t \in [0,T]$.

2. We now prove the uniqueness. By contradiction we assume there exist two solutions $\{H_1(\cdot), M_1(\cdot)\}$ and $\{H_2(\cdot), M_2(\cdot)\}$ and $H_1(t') \neq H_2(t')$ for some $t' > 0$ (we know $H_1(0) = H_2(0)$). Define $e_H = H_2 - H_1$ and $e_M = M_2 - M_1$. Using (4), we get

$$e_H(t) + e_M(t) = -\frac{c_1}{c_0}\int_0^t e_H(s)ds. \qquad (12)$$

Let $\bar{t} \leq t'$ be such that $e_H(t) \equiv 0$ for $t < \bar{t}$ and $e_H(\bar{t}) \neq 0$. By continuity of e_H, there exists $\delta > 0$ such that $e_H(t)$ has a constant sign, say, > 0 (without loss of generality), in $[\bar{t}, \bar{t}+\delta]$. Using the order preservation property of Γ (Theorem 1), $e_M(t) \geq 0$, $\forall t \in [\bar{t}, \bar{t}+\delta]$. This together with (12) leads to

$$|e_H(t)| \leq \frac{c_1}{c_0}\int_0^t |e_H(s)|ds, \forall t \in [0, \bar{t}+\delta], \qquad (13)$$

which implies $|e_H(t)| \leq 0$ by Gronwall inequality, $\forall t \in [0, \bar{t}+\delta]$, and this contradicts with $|e_H(t)| > 0$, $\forall t \in [\bar{t}, \bar{t}+\delta]$. QED.

Remark: with minor modification, we can show well-posedness of more general systems where the right hand side of the first equation in (4) is replaced by some function $f(H,u)$ continuous in u and Lipshitz continuous in H.

Continuous dependence of the solution to (4) on the parameters and the initial condition can be proved using the strong continuity property of Γ and analysis techniques for ordinary differential equations. This result is not presented here due to space limitation.

4 Parameter Identification Methods

In this section we will discuss how to identify parameters involved in (4) and (5). The experimental setup for identification and inverse control (Section 5) is shown in Figure 4. A LVDT sensor is used to measure the displacement of the actuator head.

A scheme for identification of the Preisach measure was proposed in [5]. A review of other methods for measure identification can also be found in [5]. Strictly speaking, what identified in [5] was a collection of masses sitting at centers of cells in the discretization grid. In this paper, we obtain a nonsingular Preisach measure by assuming each mass identified is distributed uniformly over the corresponding cell.

From the manufacturer, we obtained the following parameters: $N_m = 1300$, $A_m = 2.83 \times 10^{-5}\text{m}^2$, $l_m = 5.13\times10^{-2}\text{m}$, $c_0 = 1.54\times10^4\text{m}^{-1}$, $M_s = 7.87\times10^5\text{A/m}$. By applying a large input current, we estimated $\lambda_s = 0.001313$. The first resonant frequency was identified to be 392 Hz.

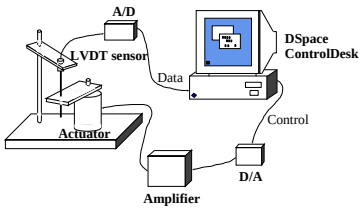

Figure 4: Experimental setup

We are now left with R_{eddy} and ξ. Generally it's impossible to write down the explicit solution of (4) in terms of R_{eddy}, therefore we can not identify R_{eddy} directly. A theoretical value of R_{eddy} can be computed with the formula $R_{eddy} = \frac{8\pi\rho N_m^2(b^2-a^2)}{l_m(b^2+a^2)}$ [19], where ρ is the resistivity of the magnetostrictive material, b and a are the outer and inner radii of the magnetostrictive rod. We use this formula to obtain a upper bound $\overline{R}$ of R_{eddy} by letting $a = 0$. We then discretize $[0, \overline{R}]$ and denote the mesh points by $R_{eddy}^{(i)}$, $i = 1, \cdots, N$. The discretization need not be uniform and we make it finer in the region where the dynamics of (4) is more sensitive to R_{eddy}.

We observe a periodic motion of the actuator head when a periodic input is applied. Numerical simulation shows that the steady-state solutions of (4) and (5) are periodic when $I(\cdot)$ is so. These observations motivate the following scheme to identify R_{eddy} and ξ:

- **Step 1.** We apply a sinusoidal current (with some dc shift) $I(\cdot)$ with frequency f to the actuator and measure the phase lag $\theta_{y,I}$ between the fundamental frequency component of the displacement and the current;

- **Step 2.** For each $R_{eddy}^{(i)}$, we numerically integrate (4) with $I(\cdot)$ as the input, and calculate the phase lag $\theta_{M^2,I}$ between the fundamental frequency component of $M^2(\cdot)$ and $I(\cdot)$.

- **Step 3.** The difference $\theta_{y,I} - \theta_{M^2,I}$ is considered to be the phase lag between the fundamental frequency component of $y(\cdot)$ and that of $M^2(\cdot)$ in (5), from which we can compute $\xi^{(i)}$.

Remarks: The idea of relating phase shift between the output and the input to hysteresis can also be found in [21]. We note that in general, the phase lag depends highly nonlinearly on initial conditions, and amplitude and frequency of $I(\cdot)$, so we should make sure that the initial conditions in simulation are consistent with experiment conditions.

Repeat the above experiment (Step 1 to Step 3) K times with different input frequencies and denote the damping coefficients as $\{\xi_k^{(i)}\}_{k=1}^K$ for $R_{eddy}^{(i)}$. If $R_{eddy}^{(i)}$ is close to the true parameter R_{eddy}, $\xi_k^{(i)}$ should not vary much with k. Therefore we pick $i^* \in \{1, \cdots, N\}$ such that $\{\xi_k^{(i^*)}\}_{k=1}^K$ has the minimum variance, and determine $R_{eddy} = R_{eddy}^{(i^*)}$ and let ξ be the mean of $\{\xi_k^{(i^*)}\}$. Figure 5 shows variation of ξ with respect to frequency for different $R_{eddy}^{(i)}$'s. The parameters are determined to be $R_{eddy} = 70\Omega$, $\xi = 0.7783$. Figure 6 compares the rate-dependent hysteresis loops measured in experiments with those obtained through simulation based on the identified parameters. We see that the simulation results agree with the experiment results reasonably well up to 200 Hz. Since the depth of eddy current penetration depends on the frequency, so does R_{eddy}. This explains why the comparison in Figure 6 goes worse when the frequency is beyond 200 Hz. In practice, one can identify R_{eddy} according to the operating frequency range of the specific application.

5 An Inverse Control Scheme

In this section we propose an inverse control scheme for the dynamical hysteresis model (4) and (5). We first formally describe the scheme to highlight the idea, then we discuss how to implement it.

Given a desired displacement trajectory $\overline{y}(\cdot) \in C^2([0,T])$, we compute for every t, $\overline{u}(t) = \frac{M_s^2}{\omega_0^2 l_m \lambda_s}(\ddot{\overline{y}}(t) + 2\xi\omega_0\dot{\overline{y}}(t) + \omega_0^2\overline{y}(t))$ and then let $\overline{M}(t) = \sqrt{u(t)}$. Next we

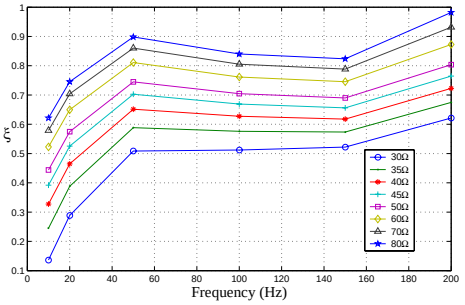

Figure 5: Identification of R_{eddy} and ξ

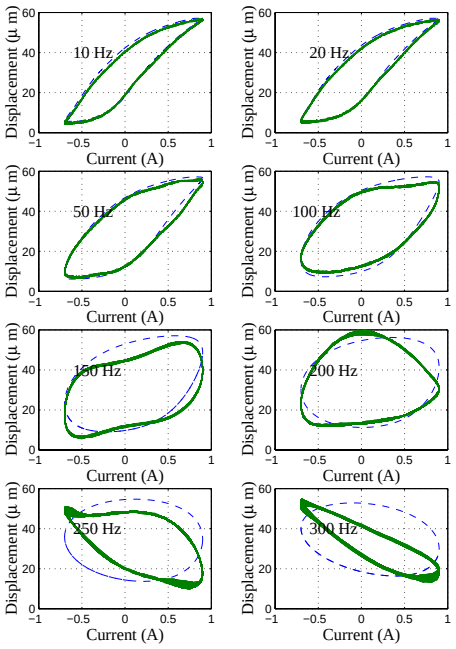

Figure 6: Model validation. Solid line: experimental measurement; Dashed line: numerical prediction

obtain $\overline{H}(\cdot)$ from $\overline{M}(\cdot)$ by inverting the Preisach operator Γ. We then (formally) let $I(t) = \frac{1}{c_1}(\dot{\overline{H}}(t) + \dot{\overline{M}}(t) + \frac{\overline{H}(t)}{c_0})$. Due to the uniqueness of solution to (4) and (5), we expect the output $y(\cdot)$ under $I(\cdot)$ to agree with $\overline{y}(\cdot)$.

However all we have just said is the ideal case. Several issues need to be taken care of in implementing the scheme:

- The desired trajectory $\overline{y}(\cdot)$ may not be twice differentiable. For (5), let $D([0,T])$ be the space of attainable $y(\cdot)$ under some control $u(\cdot) \in C([0,T])$ and $0 \le u(t) \le M_s^2, \forall t \in [0,T]$ (u plays the role of M^2 in (5)). We first need find $y^*(\cdot) \in D([0,T])$ which is closest to $\overline{y}(\cdot)$ in the sup norm (i.e., the projection of $\overline{y}(\cdot)$ in $D([0,T])$)

and then work with $y^*(\cdot)$.

- $\overline{M}(\cdot)$ or $\overline{H}(\cdot)$ may not be differentiable. In general this should not bother us because we work in the discrete time setting (for digital computer control) and the derivatives are approximated by the finite difference method.
- The closest match algorithm was proposed in [5] as an approximate inverse algorithm for the discretized Preisach operator. When the Preisach measure is assumed to be uniform in each cell on the discretized Preisach plane (see discussions in Section 4), we can develop an algorithm to compute the exact inverse of the Preisach operator Γ in the discrete time setting based on the piecewise monotonicity and the strong continuity of Γ.

Two inverse control schemes have been implemented to track a desired displacement trajectory, one based on the dynamical hysteresis model and the other based on the static hysteresis model (6). The discretization level in identification of the Preisach operator [5] was 25. Experimental results are shown in Figure 7 and 8. Instead of using some regular trajectory like sinusoids, we have obtained the desired trajectory from the output of a Van der Pol oscillator to make the tracking task more challenging. In each figure, the displacement trajectory, the tracking error and the input current used are displayed. We can see that the performance of the first scheme is very satisfactory.

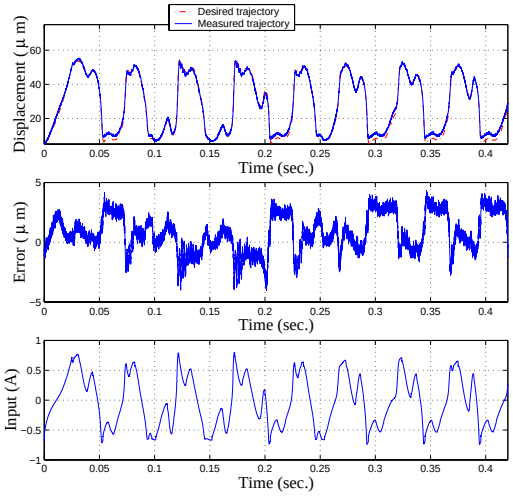

Figure 7: Inverse control based on the dynamical hysteresis model

6 Conclusions

In this paper, we have proposed a novel dynamical hysteresis model for a thin magnetostrictive actuator

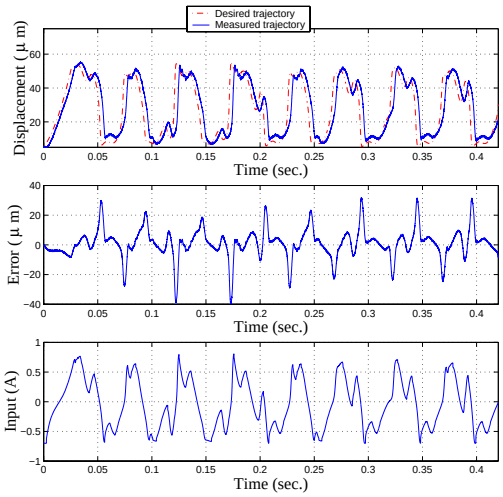

Figure 8: Inverse control based on the static hysteresis model

and proved well-posedness of the model. We have presented methods for parameter identification. Based on the model, an inverse control scheme has been developed. Experimental results have shown that the model can capture high frequency effects in the actuator, and that our identification and inverse control schemes are effective.

Due to the open loop nature of the inverse control scheme, its performance is susceptible to model uncertainty caused by parameter errors and to errors introduced by the inverse schemes. Current work involves characterizing the uncertainty and investigating robust control schemes for systems where magnetostrictive actuators are used.

7 Acknowledgment

This research was supported by the Army Research Office under the ODDR&E MURI97 Program Grant No. DAAG55-97-1-0114 to the Center for Dynamics and Control of Smart Structures (through Harvard University). We wish to thank Professor Ram Venkataraman for numerous discussions on the modeling work. It is also a pleasure to acknowledge the inspiring discussions the first author had with Professor Martin Brokate on Eq.(4) during HMM'01 at the George Washington University. Valuable comments from Professor P. S. Krishnaprasad are gratefully acknowledged.

References

[1] D. Hughes and J. T. Wen, "Preisach modeling and compensation for smart material hysteresis," in

Active Materials and Smart Structures, 1994, vol. 2427 of *SPIE*, pp. 50–64.

[2] G. Tao and P. V. Kokotović, "Adaptive control of plants with unkown hystereses," *IEEE Transactions on Automatic Control*, vol. 40, no. 2, pp. 200–212, 1995.

[3] R. C. Smith, "Inverse compensation for hysteresis in magnetostrictive transducers," *CRSC Technical Report, North Carolina State University*, CRSC-TR98-36, 1998.

[4] W. S. Galinaitis and R. C. Rogers, "Control of a hysteretic actuator using inverse hysteresis compensation," in *Mathematics and Control in Smart Structures*, V.V. Varadan, Ed., 1998, vol. 3323 of *SPIE*, pp. 267–277.

[5] X. Tan, R. Venkataraman, and P. S. Krishnaprasad, "Control of hysteresis: theory and experimental results," in *Modeling, Signal Processing, and Control in Smart Structures*, V. S. Rao, Ed., 2001, vol. 4326 of *SPIE*, pp. 101–112.

[6] C. Natale, F. Velardi, and C. Visone, "Modelling and compensation of hysteresis for magnetostrictive actuators," in *Proceedings of IEEE/ASME International Conference on Advanced Intelligent Mechatronics*, 2001, pp. 744–749.

[7] M. A. Krasnosel'skii and A. V. Pokrovskii, *Systems with Hysteresis*, Springer-Verlag, 1989.

[8] I. D. Mayergoyz, *Mathematical Models of Hysteresis*, Springer Verlag, New York, 1991.

[9] A. Visintin, *Differential Models of Hysteresis*, Springer, 1994.

[10] M. Brokate and J. Sprekels, *Hysteresis and Phase Transitions*, Springer Verlag, New York, 1996.

[11] D. C. Jiles and D. L. Atherton, "Theory of ferromagnetic hysteresis," *Journal of Magnetism and Magnetic Materials*, vol. 61, pp. 48–60, 1986.

[12] R. Venkataraman and P. S. Krishnaprasad, "A model for a thin magnetostrictive actuator," in *Proceedings of the 32nd Conference on Information Sciences and Systems*, Princeton, NJ, 1998.

[13] M. J. Dapino, R. C. Smith, and A. B. Flatau, "Structural magnetic strain model for magnetostrictive transducers," *IEEE Transactions on Magnetics*, vol. 36, no. 3, pp. 545–556, May 2000.

[14] P. Ge and M. Jouaneh, "Tracking control of a piezoceramic actuator," *IEEE Transactions on Control Systems Technology*, vol. 4, no. 3, pp. 209–216, 1996.

[15] A. A. Adly, I. D. Mayeygoyz, and A. Bergqvist, "Preisach modeling of magnetostrictive hysteresis," *Journal of Applied Physics*, vol. 69, no. 8, pp. 5777–5779, 1991.

[16] D. Hughes and J. T. Wen, "Preisach modeling of piezoceramic hysteresis; independent stress effect," in *Mathematics and Control in Smart Structures*, V.V. Varadan, Ed., 1995, vol. 2442 of *SPIE*, pp. 328–336.

[17] R. B. Gorbet, D. W. L. Wang, and K. A. Morris, "Preisach model identification of a two-wire SMA actuator," in *Proceedings of IEEE International Conference on Robotics and Automation*, 1998, pp. 2161–2167.

[18] H. T. Banks, A. J. Kurdila, and G. Webb, "Identification of hysteretic control influence operators representing smart actuators, part I: Formulation," *Mathematical Problems in Engineering*, vol. 3, no. 4, pp. 287–328, 1997.

[19] R. Venkataraman, *Modeling and Adaptive Control of Magnetostrictive Actuators*, Ph.D. thesis, University of Maryland, College Park, 1999.

[20] W. Walter, *Ordinary Differential Equations*, Springer, 1998.

[21] J. M. Cruz-Hernández and V. Hayward, "Phase control approach to hysteresis reduction," *IEEE Transactions on Control Systems Technology*, vol. 9, no. 1, pp. 17–26, 2001.